

CENTRAL GALAXIES IN DIFFERENT ENVIRONMENTS: DO THEY HAVE SIMILAR PROPERTIES?

I. LACERNA, A. RODRÍGUEZ-PUEBLA¹, V. AVILA-REESE AND H. M. HERNÁNDEZ-TOLEDO
Instituto de Astronomía, Universidad Nacional Autónoma de México, A. P. 70-264, 04510, México, D.F., México
Draft version June 10, 2018

ABSTRACT

We perform an exhaustive comparison among central galaxies from SDSS catalogs in different local environments at $0.01 \leq z \leq 0.08$. The central galaxies are separated into two categories: group centrals (host halos containing satellites) and field centrals (host halos without satellites). From the latter, we select other two subsamples: isolated centrals and bright field centrals, both with the same magnitude limit. The stellar mass (M_s) distributions of the field and group central galaxies are different, which explains why in general the field central galaxies are mainly located in the blue cloud/star forming regions, whereas the group central galaxies are strongly biased to the red sequence/passive regions. The isolated centrals occupy the same regions as the bright field centrals since both populations have similar M_s distributions. At parity of M_s , the color and specific star formation rate (sSFR) distributions of the samples are similar, specially between field and group centrals. Furthermore, we find that the stellar-to-halo mass (M_s-M_h) relation of isolated galaxies does not depend on the color, sSFR and morphological type. For systems without satellites, the M_s-M_h relation steepens at high halo masses compared to group centrals, which is a consequence of assuming a one-to-one relation between group total stellar mass and halo mass. Under the same assumption, the scatter around the M_s-M_h relation of centrals with satellites increases with halo mass. Our results suggest that the mass growth of central galaxies is mostly driven by the halo mass, with environment and mergers playing a secondary role.

Subject headings: galaxies: general – galaxies: groups: general – galaxies: halos – galaxies: statistics

1. INTRODUCTION

According to the current cosmological paradigm, galaxies form inside growing Cold Dark Matter (CDM) halos. The mass assembly of the CDM halos is hierarchical and with time many halos that were distinct (not contained inside larger halos) become subhalos. In this way, galaxies evolving in the centers of the halos and subhalos become part of gravitationally bounded groups, with a *central* galaxy residing in the center of the host halo and *satellite* galaxies residing in the orbiting subhalos.² Therefore, all observed local galaxies can be classified as centrals and satellites. One expects that the evolution of centrals is mainly driven by internal processes while the evolution of satellites is likely affected by environmental effects of the host halo, both at the dynamical (tidal stripping) and hydrodynamical (starvation, ram pressure, harassment, induced star formation, etc.) levels.

In this paper, we will focus on the properties of central galaxies of halo-based groups. It is important to highlight the differences between the classical observational definitions of groups and clusters in astronomy and the one of halo-based groups that will be used in this paper. The latter is a more general definition since it includes groups and clusters but also systems like the Milky Way and their satellites. The halo-based group concept uses

the halo radius (typically the virial one) as the criterion for defining the membership of the central and satellites galaxies to the group (see for more details Yang et al. 2005, 2007). Central galaxies in distinct halos may have many, few or no satellites above a given limit in luminosity or stellar mass. The galaxy group configuration changes actually with time, typically in the direction of the central galaxy growing by merging satellites (galactic cannibalism) and by acquiring new satellites. The observed configuration of the group, e.g., the absence of satellites or the gap between the masses (luminosities) of the central and the most massive satellite, may reveal its dynamical degree of evolution; in the context of the Λ CDM cosmology, the most massive halo-based groups (clusters of galaxies) are on average dynamically younger than the less massive ones. There emerges a natural question: is the group configuration related to the properties of the central galaxy? Are the masses, colors and star formation rates (SFR's) of centrals without satellites different from those with satellites? Among the latter, are there differences between those with small and large gaps in mass?

Among central galaxies, those in extremely isolated environments are the ones whose evolution is expected to be less affected by external physical processes. In this sense, isolated galaxies are considered as optimal objects for constraining the internal physical processes of modeled and simulated galaxies (e.g., dynamical assembly of disks and spheroids, star formation and its feedback, and AGN feedback). From the observational point of view, it is not an easy task to define optimal isolation criteria and apply them to large galaxy samples. An early attempt to construct such a sample was carried out by Karachentseva (1973), who compiled the Catalogue

¹ Also Center for Astronomy and Astrophysics, Shanghai Jiao Tong University, Shanghai 200240, China.

² The term ‘subhalos’ is sometimes used for substructures containing central or satellite galaxies. For example, in numerical simulations the main subhalo contains a central galaxy in the halo. However, in this work we refer to subhalos as the substructures that are contained inside a distinct halo and that host only satellite galaxies.

of Isolated Galaxies in the northern hemisphere (CIG) that consists of 1050 galaxies found by visual inspection of the Palomar photographic plates, with isolation criteria based on apparent diameters, projected distances, and definite size ratios between candidate isolated galaxies and potential perturber neighbors. Besides the CIG and its recent refinements (see below), other catalogs with different isolation criteria have been compiled and used as control samples in studies of galaxies in different environments (Márquez et al. 1999; Aars et al. 2001; Varela et al. 2004; Verley et al. 2007, among others).

The CIG is a magnitude-limited sample that is approximately complete up to $m_{ZW} \sim 15.5$ (blue magnitudes) with a well defined selection function. After the extensive homogeneous spectroscopic and imaging data releases from digitized sky surveys, several works improved the observational properties of the objects in the CIG catalog (e.g., Verdes-Montenegro et al. 2005; Hernández-Toledo et al. 2007, 2008). In Hernández-Toledo et al. (2010) the isolation criterion has been refined to include information on the relative recessional velocities of the galaxies and their neighbors (a 3D selection instead of a 2D-isolation criterion) as an attempt to avoid non-physical (projected) companions. These authors have applied the refined CIG isolation criteria to the Sloan Digital Sky Survey (SDSS) DR5 (Adelman-McCarthy et al. 2007) and found 1520 isolated galaxies above 15.2 r -band apparent magnitudes in the sample dubbed as UNAM-KIAS.

We analyze the properties of central galaxies from the Yang et al. (2007, hereafter Y07) halo-based group catalog and from the isolated UNAM-KIAS catalog. We can separate the Y07 sample into centrals with satellites and those with not detected satellites (the only galaxy in the halo is the central one). In addition, we select those centrals which correspond to very isolated galaxies in the UNAM-KIAS catalog. It is known that satellite galaxies show properties that are different when compared to central galaxies mainly due to environmental effects of the host halo (e.g., Weinmann et al. 2006; van den Bosch et al. 2008; Weinmann et al. 2009; Pasquali et al. 2010; Peng et al. 2010, 2012; Woo et al. 2013; Wetzel et al. 2013, and more reference therein). Our aim is to explore the differences in properties among centrals with a massive satellite, with smaller satellite(s), without satellites, and in very isolated environments. This exercise is important for evaluating the use of central and isolated galaxies as control objects in studies aimed to constrain galaxy evolution driven by internal physical processes.

The outline of this work is as follows. In Section 2, we present the data set of central galaxies studied in this work. We compare observational properties such as color and specific SFR among the different categories of central galaxies in Section 3. In Section 4, we study the stellar-to-halo mass relation of central galaxies, with an emphasis on how this relation depends on the properties of very isolated galaxies. We discuss our results in Section 5. Finally, in Section 6, we give our conclusions.

2. DATA

The aim of this paper is to analyze the properties of central galaxies in different environments. For this purpose, we use the general galaxy group catalog con-

structed by Y07 and the catalog for isolated galaxies reported in Hernández-Toledo et al. (2010). We select the central galaxy as the most massive object within the halo. This seems to be a reasonable assumption for halos less massive than $\sim 2 \times 10^{13} M_{\odot}$ (which is our general case; see the bottom panel of Fig. 9 below). According to a study carried out by Skibba et al. (2011), the fraction of most massive galaxies which are not the centrals in these halos is ~ 0.25 . This fraction increases to ~ 0.4 for the most massive halos.

The first catalog is extracted from a more general galaxy group sample constructed by Y07 from the New York University Value-Added Galaxy Catalog (NYU-VAGC; Blanton et al. 2005), which is based on SDSS DR4 (Adelman-McCarthy et al. 2006). By using a halo-based group finder algorithm, Y07 (see also Yang et al. 2008, 2009, 2012) associated dynamically to the galaxies a dark matter halo. This group system may contain one or more galaxies and extends up to the virial radius of the given halo. The idea behind the group finder consists of an iterative procedure that uses average mass-to-light ratios of groups, based on the total luminosity of all group members down to some luminosity, to assign a tentative mass to each group. Then the virial radius associated to this mass is used to recalculate the group membership, repeating this process until convergence is reached. Y07 have tested this method by constructing mock catalogs based on the SDSS and found that 80% have a completeness greater than 0.6, while 85% have a contamination by interlopers lower than 0.5. The full sample consists of 369 447 galaxies with redshifts in the range $0.01 \leq z \leq 0.2$, where the $\sim 80\%$ of them are central galaxies. Hereafter we refer to central galaxies in halos without satellites as *field centrals*, $N = 1$, and those central galaxies in halos that host satellites as *group centrals*, $N > 1$, where N is the total number of galaxies within a halo.

Since fiber collisions could introduce some systematic error in the Y07 group identification algorithm, it is important to study its impact. To that end, Yang et al. (2009) divided the group catalog into two samples: one that uses galaxies with known redshifts and another that includes galaxies which lack redshifts due to fiber collisions. They found that the conditional stellar mass function for the fiber collision-corrected sample has a higher amplitude than that in the non-corrected case, particularly for low-mass halos. Nevertheless, the differences are marginal and well within the error bars. Therefore, we conclude that fiber collisions in the Y07 sample are not a source of systematic errors that could affect our conclusions.

The second catalog comes from the UNAM-KIAS collaboration (Hernández-Toledo et al. 2010). They identified a total of 1520 isolated galaxies from the SDSS DR5 using an improved method based on the 2D-criterion of isolation proposed by Karachentseva (1973). In addition to the condition that the projected separation from a neighbor across the line of sight is greater than 100 times the seeing-corrected Petrosian radius of the neighbor galaxy, the new method takes into account that the radial velocity difference with respect to a neighbor is greater than 1000 km s^{-1} to mimic a 3D-criterion. The velocity information on galaxies in the radial direction is used to tackle projection effects as much as possible. In cases when a candidate (isolated) galaxy has close

neighbors (i.e., it does not satisfy the 3D-criterion), this galaxy can be considered as isolated if the extinction-corrected apparent Petrosian r -band magnitude difference between the candidate galaxy and any neighbor is 2.5 mag ($\Delta m_r \geq 2.5$). This condition allows an isolated galaxy to have close (and fainter) neighbors but rejects relevant perturbers. As the magnitude limit of SDSS is $m_r \sim 17.7$, only galaxies brighter than $m_r = 15.2$ were used to select isolated galaxies to take into account the magnitude difference of $\Delta m_r \geq 2.5$. Most of the isolated galaxies have a redshift distribution between $z \sim 0$ and $z \sim 0.08$, with a mean redshift of $\langle z \rangle = 0.032$. After using an image processing scheme, the catalog contains the information on several structural parameters, including the morphological parameter T . For more details regarding the UNAM-KIAS catalog see Hernández-Toledo et al. (2010).

In general isolated galaxies are central objects within their host halos, although a small fraction of them can be satellite galaxies residing in the outskirts of parent halos (Hirschmann et al. 2013). Formally, we define our sample of isolated central galaxies as the intersection of the UNAM-KIAS catalog with the one of field centrals ($N = 1$) in the Y07 catalog. There are 1046 isolated galaxies from UNAM-KIAS in Y07. The rest of isolated galaxies were not identified because of the different redshift distributions of both catalogs (see Section 2.1) or because they belong to different data releases. We excluded from our study 4 out of 1046 isolated galaxies which are classified as satellites in Y07 according to their stellar mass (one of them is the central object according to their luminosity, other two galaxies are located in the outskirts of relatively massive groups and the remaining isolated satellite galaxy resides within a halo that suffers strong survey edge effects). We found other 220 isolated galaxies which are centrals in groups that host satellites ($N > 1$). Recall that the isolation criterion requires not to have companions more luminous than 2.5 mag the apparent magnitude of the primary; galaxies with fainter companions (i.e., satellites) than this threshold are considered as isolated objects. We find that 85% of the 220 isolated galaxies in halos with satellite(s) according to Y07, have their most massive satellite below 0.1 times the mass of the central. Therefore, these satellites are likely considered as not relevant perturbers by the isolation criterion of the UNAM-KIAS collaboration. On the other hand, note that the group finder algorithm of Y07 suffers a contamination of around 10% when classifying centrals and satellites. Rigorously, we decided to exclude from our analysis those 220 isolated central galaxies that appear with satellite(s) in the Y07 catalog. There remain then 822 isolated galaxies that are centrals in halos with no satellites ($N = 1$) in Y07. These galaxies conform our robust *isolated central* galaxy sample.

Since the sample of isolated central galaxies is brighter than $m_r = 15.2$, we impose the same apparent magnitude limit on the field central galaxy sample in order not to introduce a selection bias when making comparisons among them. We refer to this subsample as the *bright field centrals*. Recall that the central galaxies without satellites can be located in a wide range of environments, including the very isolated one. The isolated galaxies are actually those (bright) field centrals obeying extreme isolation criteria. Based on these criteria, we conclude

that the subsample of isolated galaxies differs in its local environment from the bulk of the bright field centrals. Our subsample of isolated centrals is in fact an extreme of the distribution of all field central galaxies regarding environment.

2.1. Volume and mass limits

Since the UNAM-KIAS catalog reaches mainly out to $z = 0.08$ and Y07 catalog ranges from $z = 0.01$ out to $z = 0.2$, we select those galaxies that are located within the same volume in redshift space in order to have a fair comparison between central galaxies from both catalogs. Therefore, throughout the text we use the redshift range $0.01 \leq z \leq 0.08$. As explained below, we characterize the galaxies from all of our samples by their stellar mass, M_s . In a magnitude limited sample, the minimum detected M_s depends on the redshift and on the stellar mass-to-luminosity ratio; the latter depends on the stellar populations and therefore on galaxy colors. For the SDSS sample and its magnitude limit, van den Bosch et al. (2008, see also Yang et al. 2009) have calculated the stellar mass limit at each z above which the sample is complete, i.e., galaxies are potentially observable above this mass:

$$\log[M_{s,lim}/h^{-2} M_\odot] = \frac{4.852 + 2.246 \log(d_L) + 1.123 \log(1+z) - 1.186z}{1 - 0.067z}. \quad (1)$$

We adopt this limit.

After imposing the above mentioned volume and mass limits to our samples, there remain 822 isolated, 10 708 group, 40 551 field and 4358 bright field central galaxies. These are the main samples to be used in this paper. A summary of their properties is given in Table 1.

2.2. Stellar and gas masses, colors and sSFR

In Section 3 we will compare observational properties such as color and specific star formation rate (sSFR) in bins of stellar mass (M_s) for our samples of central galaxies. Details of these properties are given in this Section.

Stellar masses for all the central galaxies are taken from Y07, who used the relation between the stellar mass-to-light ratio and color of Bell et al. (2003). We note that in the processed MPA-JHU DR7 catalog,³ stellar masses are also provided for each galaxy in the Y07 group catalog, but calculated in this case through the spectral energy distribution fitting. While this method offers a more constrained estimate for the stellar masses than the Bell et al. (2003) method, the differences between the two mass estimates are small and not systematical (see for a comparison e.g., Dutton et al. 2011).

For the isolated central galaxies, we are also interested in the study of how their gas content compares with respect to observations. We include the information on the H I line magnitude (corrected for self-absorption) from the HyperLeda database⁴ for the sample of isolated galaxies in order to estimate their gas mass M_{gas} content. The neutral hydrogen line magnitude in 21 cm, m_{21} , is converted into H I mass M_{HI} by using

$$\frac{M_{HI}}{M_\odot} = 2.36 \times 10^5 d_L^2 10^{(17.4 - m_{21})/2.5}, \quad (2)$$

³ Available at <http://www.mpa-garching.mpg.de/SDSS/DR7/>

⁴ <http://leda.univ-lyon1.fr/>

TABLE 1
GENERAL PROPERTIES OF THE CENTRAL GALAXY SAMPLES

sample	N	source catalog	z -range	m_r limit	n	n_{M_h}
(1)	(2)	(3)	(4)	(5)	(6)	(7)
group	> 1	Y07	$0.01 \leq z \leq 0.08$	< 17.77	10708	9271
field	= 1	Y07	$0.01 \leq z \leq 0.08$	< 17.77	40551	28043
bright field ^a	= 1	Y07	$0.01 \leq z \leq 0.08$	< 15.2	4358	3420
isolated ^b	= 1	UNAM-KIAS	$0.01 \leq z \leq 0.08$	< 15.2	822	663

NOTE. — Column 1: sample name. Column 2: galaxy number within the host halo. Column 3: source catalog. Column 4: redshift range. Column 5: extinction-corrected apparent Petrosian r -band magnitude limit. Column 6: galaxy number of each sample. Column 7: number of galaxies with halo mass estimates.

^aSubsample of the field central galaxies with $m_r < 15.2$.

^bIsolated galaxies identified in the bright field sample.

where d_L is the luminous distance in Mpc (Roberts & Haynes 1994) which is calculated under the Λ CDM cosmology with $\Omega_m = 0.27$, $\Omega_\Lambda = 0.73$. The gas mass can be calculated by using a simple correction for helium and metals, $M_{gas} = 1.4M_{HI}$, or, more accurately, by adding a correction for the molecular hydrogen H_2 , $M_{gas} = 1.4M_{HI}(1 + M_{H_2}/M_{HI})$. The ratio M_{H_2}/M_{HI} depends on the morphological parameter T , which is available in the UNAM-KIAS catalog. This ratio is given by $M_{H_2}/M_{HI} = 3.7 - 0.8T + 0.043T^2$ (McGaugh & de Blok 1997). As noted by Avila-Reese et al. (2008), this empirical relation is valid for late-type spiral galaxies ($T \geq 2$) since it can overestimate the gas mass for galaxies with earlier morphologies. For galaxies with $T < 2$, we use their assumption $M_{H_2}/M_{HI} = 2.3$.

In Section 3 we use two widely separated bands for the color, namely $g - i$. The $g - i$ color is measured using *modelMag* magnitudes of SDSS corrected for extinction (*dered* parameter in CasJobs).⁵ This magnitude is defined as the better of two magnitude fits; a pure de Vaucouleurs profile and a pure exponential profile. The inclination of the galaxies combined with dust extinction in the disk produces a systematic reddening of their colors. In order to ameliorate this systematic effect, throughout this paper we will not use the colors of those galaxies with inclination angles higher than 70 degrees. The inclination angle *inc* is calculated as $\cos(\text{inc}) = b/a$, where b/a is the r -band minor-to-major isophotal axis ratio from SDSS.

Finally, we include in our samples the sSFR, defined as the SFR divided by the stellar mass. This quantity has been obtained from the MPA-JHU DR7 catalog, and it is an updated version of the estimates presented in Brinchmann et al. (2004) by using a spectral synthesis fitting model.

2.3. Halo mass

The Y07 group catalog includes by construction the halo (virial) mass, M_h , of the central galaxies down to some luminosity. This kind of halo-based group finders have emerged as a powerful method for estimating group halo masses, even when there is only one galaxy in the group halo. By using mock catalogs that resemble observations, it has been shown that the group masses estimated with this method can recover successfully the true halo mass, in a statistical sense, with no significant systematics (Yang et al. 2008). It was also shown that

most of the scatter in the relation between the true and assigned halo masses in the mock catalog is owed to the intrinsic scatter; the fact that the group finder is not perfect, i.e., suffers from interlopers and incompleteness, and that it is necessary to correct the characteristic luminosity for members that do not make the magnitude limit of the survey, only adds a relatively small contribution to the total scatter.

The Y07 catalog contains the halo membership, the identification of central and satellite galaxies in the halo, and M_h based on either the characteristic stellar mass or the characteristic luminosity in the group, among other halo properties. We use the halo mass based on the characteristic stellar mass. The characteristic stellar mass (luminosity) is defined as the sum of the stellar mass (luminosity) of all the galaxies in the halo with $^{0.1}M_r - 5 \log(h) \leq -19.5$, where $^{0.1}M_r$ is the absolute magnitude in the r -band with K -correction and evolution-correction at $z = 0.1$. It is also considered the completeness of the survey at the redshift of each of these galaxies, as well as a correction factor for the apparent magnitude limit of the spectroscopic survey. They assume a one-to-one relation between the characteristic stellar mass (luminosity) and M_h by matching their rank orders for a given volume and a given halo mass function.

The obtained M_s - M_h relation is robust: by using it in mock catalogs, the average relations of halo occupation statistics are recovered (Y07). This approach has advantages in a statistical sense over other methods used for estimating group (halo) masses, such as the one based on velocity dispersions, that needs a significant number of members to calculate dynamical masses, or the gravitational lensing or X-ray emission method, that need data of high quality which are applied only to massive systems. However, for groups/single-galaxy systems which are not complete in characteristic stellar mass (luminosity), the halo mass estimates under the assumption of the one-to-one relation mentioned above are already not reliable; thus, the central galaxies fainter than the magnitude limit do not have halo mass estimates. This is why the halo mass limit in the Y07 catalog is $10^{11.6}h^{-1} M_\odot$. Nonetheless, we note that due to the method used in Y07 the estimated halo masses are not measurements of the true halo masses. In addition, groups with strong survey edge effects do not have halo mass estimates regardless the luminosity of their members. The latter affects only 1.6% of all Y07 groups. The number of central galaxies with host halo masses is smaller than in the original catalog. For the samples used here, those with estimated halo masses are reduced in number to 663 isolated, 9271

⁵ See <http://casjobs.sdss.org/CasJobs/>

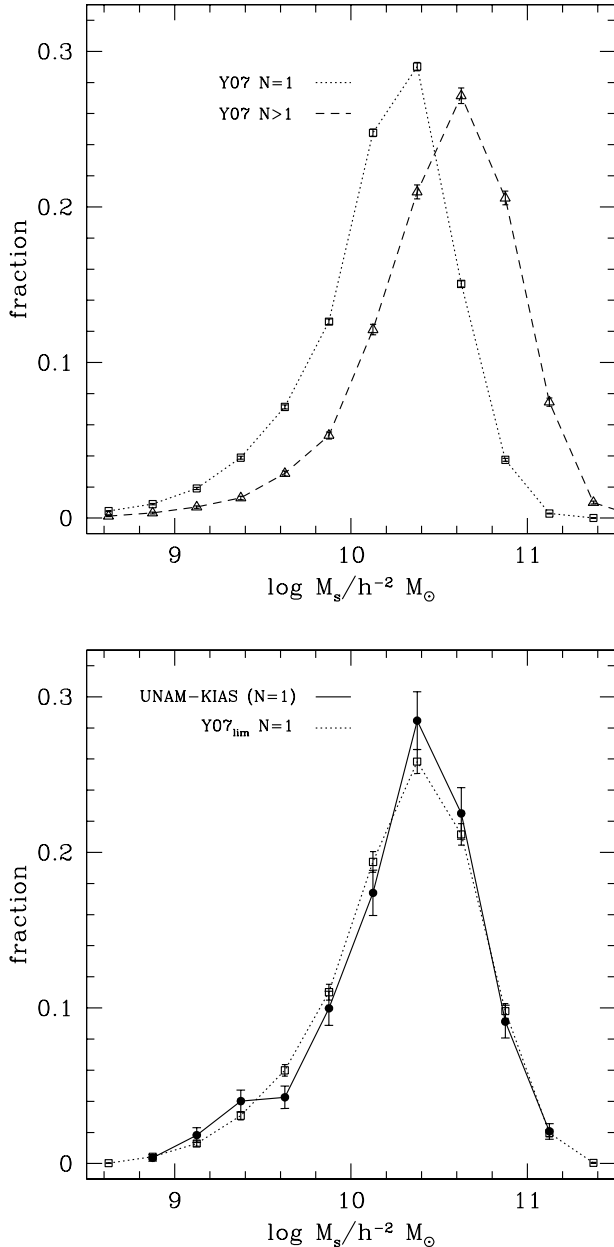


FIG. 1.— Relative fraction of central galaxies as a function of stellar mass. The sum of the points for each category is equal to unity, therefore each line may be considered as a probability distribution. The error bars correspond to the Poisson error. Top panel: field and group galaxies (open squares and open triangles connected by dotted and dashed lines, respectively). At high masses, the fraction of group centrals dominates with respect to that of field central galaxies. Bottom panel: isolated and bright field galaxies (filled circles and open squares connected by solid and dotted lines, respectively). Both distributions are similar within the errors.

group, 28 043 field and 3420 bright field central galaxies (see Table 1). These samples will be used in Section 4.

3. OBSERVATIONAL PROPERTIES

As mentioned above, we define four categories of central galaxies (see Table 1). The first two categories are the *group centrals* (host halos with $N > 1$) and *field centrals* (host halos with $N = 1$, i.e., no satellites). The

former makes the 21% of all central galaxies of our local ($0.01 \leq z \leq 0.08$) Y07 sample, whereas the latter form the 79%. The field centrals can inhabit all kinds of environments (e.g., around groups or clusters, along a filament, within a void or simply close to other galaxies), excepting those with other galaxies within their virial radius, i.e., groups and clusters of galaxies. Thus, for field central galaxies it is also possible that their near environment might be playing an important role in shaping their properties. In order to select field centrals in extreme isolated environments we use the *very isolated central* sample (taken from the UNAM-KIAS catalog and identified in the Y07 catalog). Since the isolated sample has a brighter magnitude limit than the field sample, we avoid a selection bias when comparing both samples by using the *bright field central* subsample, i.e., those field galaxies selected with the same m_r limit that the UNAM-KIAS catalog (Section 2). The isolated galaxies make the 19% of the bright field sample. The aim of this work is to study and compare the properties of central galaxies selected from the group, field, and isolated samples.

Our samples are not complete in the sense of observing the full distribution of galaxies above a given (small) mass (e.g., see the drop in the fraction of low-mass galaxies in Fig. 1). In fact, we will not deal with stellar mass functions, where corrections like the V/V_{max} should be introduced. We only compare samples in the same redshift ranges that satisfy the stellar mass completeness condition provided by van den Bosch et al. (2008, eq. 1).

The top panel of Fig. 1 shows the relative fraction of field and group central galaxies as a function of stellar mass (dotted and dashed lines, respectively). Each distribution is normalized and can be considered as a probability distribution. Since both samples are from the same parent volume-limited sample ($0.01 \leq z \leq 0.08$), the comparison among them in Fig. 1 is fair in the sense that any incompleteness due to not observed galaxies is expected to be the same for them. The differences among the samples of field and group central galaxies in the stellar mass distribution is noticeable. In addition, we performed a chi-square test, which is useful for binned data (Press et al. 1992), that confirms a very low probability of $P < 4 \times 10^{-4}$ that both normalized distributions are similar. The fraction of field centrals at low masses, $M_s < 10^{10} h^{-2} M_\odot$, is higher than the fraction of group centrals. At higher stellar masses, $M_s > 4 \times 10^{10} h^{-2} M_\odot$, the relative fraction of group centrals is higher than that of field centrals. Around 56% of group central galaxies ($N > 1$) are found at these high masses, whereas this percentage decreases to 19% for field centrals ($N = 1$). The top panel also shows that the distributions of the centrals peak at different masses: field centrals at ~ 10.4 and group centrals at 10.6 in $\log(M_s/h^{-2} M_\odot)$.

In the same figure, the bottom panel shows the relative fraction of isolated and bright field central galaxies as a function of stellar mass. There are no significant differences between both distributions within the errors; the chi-square test confirms this with a probability $P = 0.999$. Both distributions peak at $\log(M_s/h^{-2} M_\odot) \sim 10.4$. This similarity in the mass distributions suggests that the way central galaxies without satellites ($N = 1$) attained their final stellar mass does not depend signif-

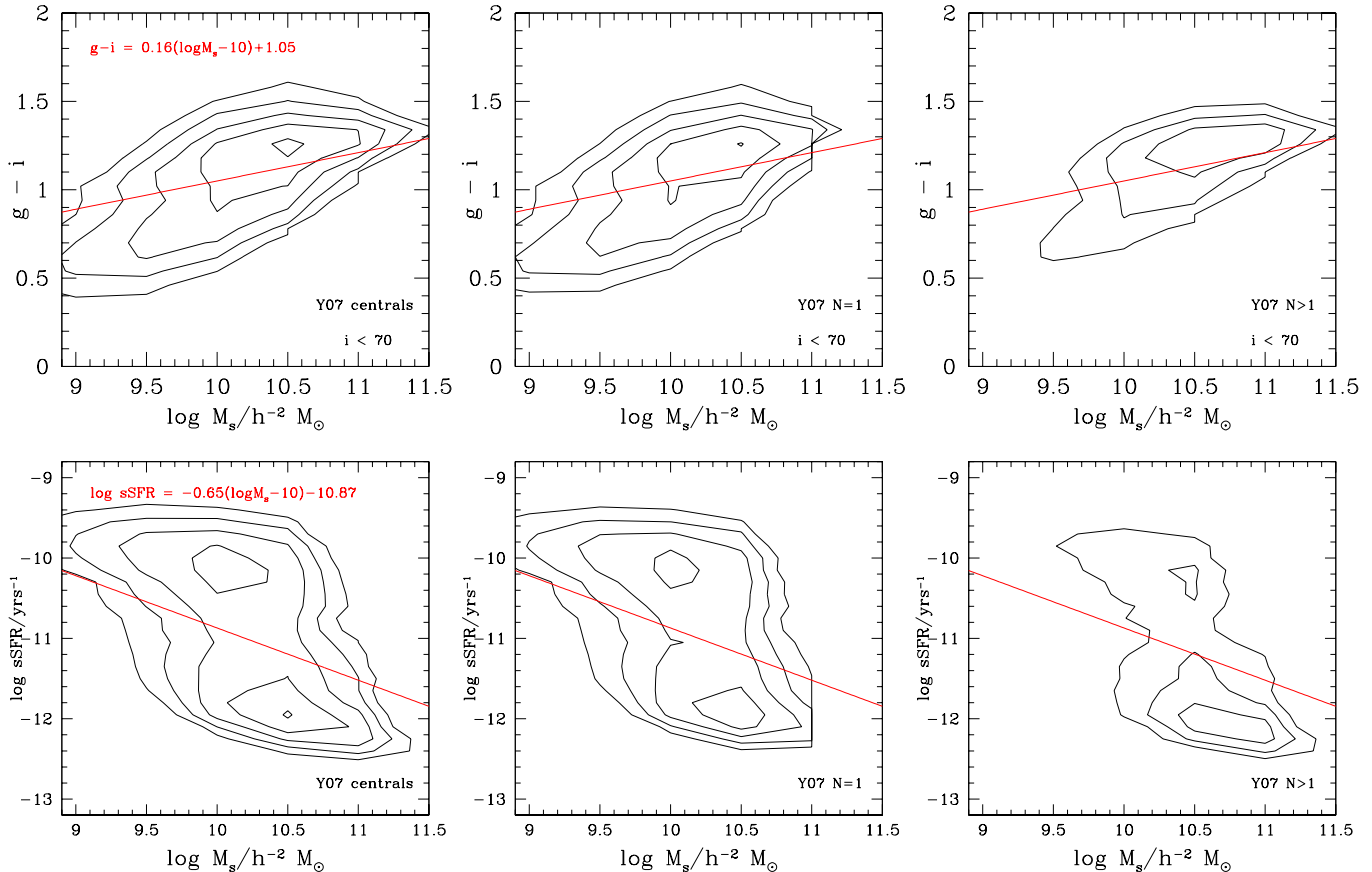


FIG. 2.— Color ($g - i$, top panels) and specific star formation rate (bottom panels) as a function of stellar mass. All the central galaxies between $0.01 \leq z \leq 0.08$ are shown in contours in the left column. They are split in field ($N = 1$, middle column) and group ($N > 1$, right column) central galaxies. Concerning colors, we do not include objects with inclinations above 70 degrees. The red lines in the top and bottom panels show equations (3) and (4) to separate red/blue and passive/active galaxies, respectively.

icantly on the environment further away from the halo virial radius, at least for these bright ($m_r < 15.2$) galaxies.

Figure 2 shows the $g - i$ color (top panels) and sSFR (bottom panels) vs. the stellar mass. The left panels include all the central galaxies between $0.01 \leq z \leq 0.08$ distributed in iso-contours of number density increasing by 0.5 dex. We observe that the distributions of $g - i$ color and sSFR depend on the stellar mass, where the bimodality in the latter is more marked than the former. Therefore, we can separate galaxies in red/blue and passive/active by using

$$g - i = 0.16[\log(M_s) - 10] + 1.05 \quad (3)$$

$$\log(\text{sSFR}) = -0.65[\log(M_s) - 10] - 10.87, \quad (4)$$

where M_s is in units of $h^{-2} M_\odot$ and sSFR is in units of yr^{-1} .⁶ These equations are shown as red solid lines. The iso-contours in the middle and right columns correspond to the samples separated into field ($N = 1$) and

⁶ These mass-dependent criteria for separating galaxies into two groups, active/passive or blue/red, have been obtained by fitting two Gaussians to the corresponding (color or sSFR) distributions at different mass bins (see Figs. 3 and 4 below) and choosing the $g - i$ or sSFR values at the given bin as the ones where both Gaussians intersect in each case.

group ($N > 1$) central galaxies. As can be seen in the top panels, the field centrals populate both the blue cloud and red sequence regions, with a preference for the former, whereas the group centrals are strongly biased to the red sequence. Recall that we do not consider galaxies with high inclination angles ($inc > 70$ degrees) in order to avoid systematic effects of reddening by extinction. The left-bottom panel of Fig. 2 shows the sSFR as a function of stellar mass of all the central galaxies out to $z = 0.08$, which is similar to the one presented in Yang et al. (2013) by using a central galaxy sample out to $z = 0.2$. In the middle-bottom and right-bottom panels we present the same but for field and group centrals, respectively. We find that the distribution of field central galaxies is strongly bimodal, whereas the distribution of group central galaxies shows a higher preference for occupying the passive region. Only a small fraction of group centrals are star forming galaxies.

We thus conclude that field and group central galaxies show different distributions in the color- M_s and sSFR- M_s diagrams. Central galaxies in halos without satellites ($N = 1$; field) seem to be bluer and more star forming than centrals located in halos which host satellites galaxies ($N > 1$; group). In fact, such differences can be explained by their differences in the stellar mass distributions. Typically, group central galaxies have higher stellar masses than field central galaxies (top panel of

TABLE 2
RELATIVE FRACTIONS OF BLUE FIELD AND BLUE GROUP CENTRAL GALAXIES

$\log M_s$	$g-i$ cut	f_{blue} field	f_{blue} group
9.2–9.6	0.95	0.79	0.84
9.6–10.0	1.02	0.65	0.67
10.0–10.4	1.08	0.31	0.33
10.4–10.8	1.15	0.18	0.21
10.8–11.2	1.21	0.12	0.13

NOTE. — Stellar mass bins as shown in Fig. 3. The second column indicates the cut in $g-i$ to define a blue/red galaxy.

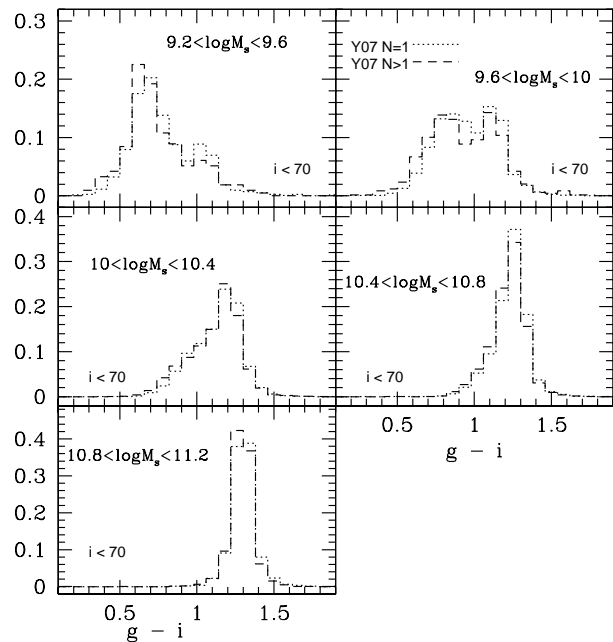


FIG. 3.— Histograms of $g-i$ color for field ($N = 1$; dotted lines) and group ($N > 1$; dashed lines) central galaxies for different stellar mass bins. The stellar mass M_s is in units of $h^{-2} M_\odot$. We do not include objects with high inclination (angles over 70 degrees). Each histogram was normalized by the total number of selected objects, so that the sum of each distribution is equal to unity.

Fig. 1). Therefore, considering the overall populations, group centrals are redder, with a significant red sequence, and more passive than field centrals. We also compare the samples of isolated and bright field centrals in the color- M_s and sSFR- M_s diagrams. As expected, both samples occupy the same regions because of their similar stellar mass distributions (bottom panel of Fig. 1).

We have found differences among central galaxies, which can be explained mainly by the differences in their stellar mass distributions. In the next subsections we will compare the properties of central galaxies in stellar mass bins. We begin by comparing the $g-i$ color and the sSFR distributions between the samples of field and group central galaxies. Then, in order to test whether central galaxies are affected by more extreme environmental effects, we will repeat our analysis between the subsamples of isolated galaxies and bright field central galaxies.

3.1. Field and group central galaxies

Fig. 3 shows a series of $g-i$ color histograms for field ($N = 1$; dotted lines) and group ($N > 1$; dashed lines)

TABLE 3
RELATIVE FRACTIONS OF ACTIVE FIELD AND ACTIVE GROUP CENTRAL GALAXIES

$\log M_s$	sSFR cut	f_{active} field	f_{active} group
9.2–9.6	-10.5	0.82	0.84
9.6–10.0	-10.7	0.71	0.70
10.0–10.4	-11.0	0.53	0.52
10.4–10.8	-11.3	0.33	0.31
10.8–11.2	-11.5	0.14	0.11

NOTE. — M_s bins as shown in Fig. 4. The second column is the cut in $\log(\text{sSFR}/\text{yrs}^{-1})$ to define an active/passive galaxy.

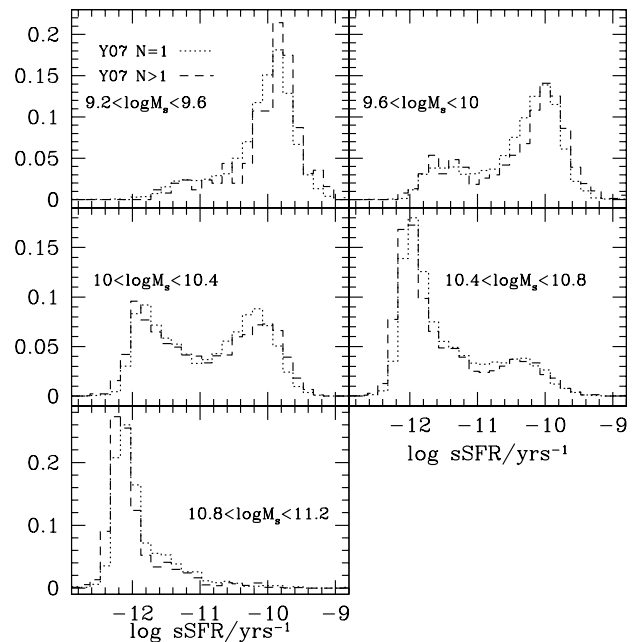


FIG. 4.— Histograms of sSFR for field ($N = 1$; dotted lines) and group ($N > 1$; dashed lines) central galaxies for different stellar mass bins. The stellar mass M_s is in units of $h^{-2} M_\odot$. Each histogram was normalized by the total number of selected objects, so that the sum of each distribution is equal to unity.

central galaxies in different stellar mass bins. Each distribution is normalized so that its sum is equal to unity. At a qualitative level, we see that there are no significant differences in the color distributions between both populations at a given stellar mass. The chi-square test confirms with a very high probability ($P > 0.999$) that both normalized distributions are similar in each panel. Table 2 reports the corresponding fractions of blue central galaxies, f_{blue} (the complement is the fraction of red centrals, $f_{red} = 1 - f_{blue}$) in stellar mass bins as shown in Fig. 3. The criterion to define blue and red galaxies is the one given in eq. (3). For low-mass galaxies (top panels), most of them are blue, though a small population of redder galaxies appears (slight bimodality). We measure that the fraction of red group centrals is at most 5% lower than that of red field centrals. At intermediate masses (middle panels), the slight bimodality disappears, and both populations are typically red. Similarly, for high-mass galaxies (bottom panel), nearly all the field and group central galaxies are red with the peak around $g-i = 1.3$.

Fig. 4 shows the same as Fig. 3 but for the sSFR.

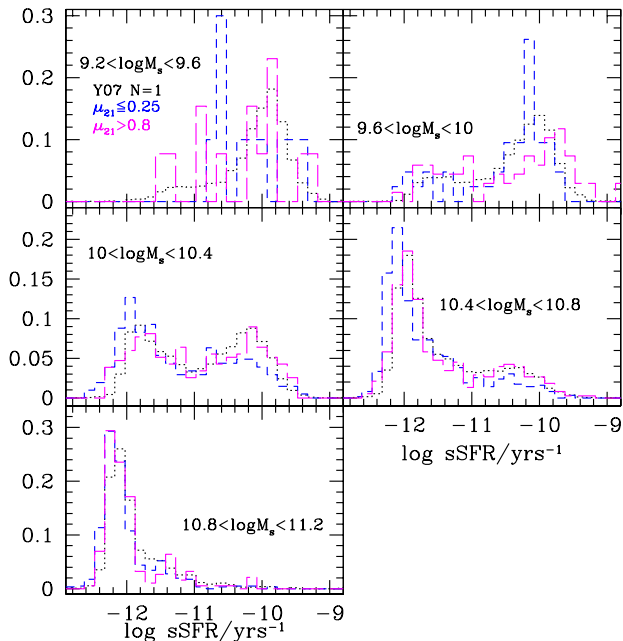


FIG. 5.— Same as Fig. 4, but the group central galaxies ($N > 1$) are split according to the stellar mass ratio, μ_{21} , between the most massive satellite and the group central galaxy. Blue dashed and magenta long-dashed lines correspond to ratios lower than 0.25 and higher than 0.8, respectively. Each histogram was normalized by the total number of selected objects, so that the sum of each distribution is equal to unity. The fraction of passive/active central galaxies with $N > 1$ depends on the μ_{21} value. Central galaxies with $\mu_{21} > 0.8$ (i.e., their most massive satellite has a comparable stellar mass) are slightly more active.

Analogously to the color distributions, there are not significant differences in this property between group and field central galaxies (the chi-square test confirms a very high probability, $P > 0.998$, that both normalized distributions are similar in each panel). In Table 3 we report the corresponding fractions of active central galaxies, f_{active} (the complement is the fraction of passive centrals, $f_{passive} = 1 - f_{active}$) in M_s bins as shown in Fig. 4. The bimodality in sSFR is more evident for intermediate masses (middle panels). In the mass range $10 < \log(M_s/h^{-2} M_\odot) < 10.4$, group central galaxies show two strong peaks (the active and passive populations), where the peak of active galaxies is slightly lower than that of passive objects. In the case of field central galaxies, the active and passive populations exhibit similar peaks. However, the fractions of active group centrals and active field centrals are very similar (52% and 53%, respectively). For high-mass galaxies (bottom panel), most of the galaxies are passive.

We further explore the possibility of some systematic variation in the color and sSFR for the group centrals as a function of the mass ratio with respect to the most massive satellite. The presence of a massive neighbor satellite galaxy is expected to increase the probability of triggering star formation activity in the central galaxy. We select those group centrals ($N > 1$) according to the stellar mass ratio between the most massive satellite and the central galaxy (i.e., the mass ratio between the second most massive and the most massive galaxy within the halo, μ_{21}). We only choose systems where the most mas-

TABLE 4
RELATIVE FRACTIONS OF BLUE BRIGHT FIELD AND BLUE ISOLATED CENTRAL GALAXIES

$\log M_s$	$g - i$ cut	f_{blue}	bright field	f_{blue} isolated
9.2–9.7	0.96	0.90	0.91	
9.7–10.2	1.04	0.70	0.76	
10.2–10.7	1.12	0.48	0.55	
10.7–11.2	1.20	0.34	0.35	

NOTE. — M_s bins as shown in Fig. 6. The second column indicates the cut in $g - i$ to define a blue/red galaxy.

sive satellite is complete in stellar mass by means of eq. (1). The distribution of μ_{21} for the selected sample has a broad maximum at ≈ 0.25 , and correlates weakly with the stellar mass in the sense that the smaller the value of μ_{21} , the larger the M_s of the group central galaxy (for extensive results on this kind of dependence on M_s and M_h see Yang et al. 2008; Rodríguez-Puebla et al. 2013. For similar results but with dependence on luminosity see More 2012; Hearin et al. 2013).

We note that the $g - i$ color distributions in different mass bins do not differ between those group central galaxies with $\mu_{21} > 0.8$ and $\mu_{21} \leq 0.25$. In contrast, as can be seen in Fig. 5, small differences are found in the distributions of sSFR for group centrals in terms of μ_{21} , in particular in the mass interval $9.6 < \log(M_s/h^{-2} M_\odot) < 10.4$. The group central galaxies ($N > 1$) are split into two subsamples: $\mu_{21} \leq 0.25$ (blue dashed lines) and $\mu_{21} > 0.8$ (magenta long-dashed lines). In general, from the figure we see that the overall fraction of active/passive central galaxies with $N > 1$ depends on the value of μ_{21} . Active group central galaxies with $\mu_{21} > 0.8$ have slightly higher sSFR values than those with $\mu_{21} \leq 0.25$ since they peak at higher sSFR values. The fraction of active centrals with $N > 1$ is around 51% for the mass ratio $\mu_{21} > 0.8$, while for the mass ratio $\mu_{21} \leq 0.25$ this fraction is 38% at the mass bin $10.0 < \log(M_s/h^{-2} M_\odot) < 10.4$ (left-middle panel). This suggests that central galaxies with high-mass ratios μ_{21} might have enhanced their star formation activity, most likely induced by their massive satellites.

It is worth noting that in the case of sSFR, the bimodality is well established for all central galaxies at the $\sim 1 - 5 \times 10^{10} h^{-2} M_\odot$ masses, while the $g - i$ color distributions in most of the mass bins are hardly bimodal (an incipient bimodality is seen for $M_s < 10^{10} h^{-2} M_\odot$). For intermediate-mass central galaxies, a fraction of 70–80% are red and 30–50% are active, thus one expects a non-negligible fraction of red but currently star forming central galaxies. In Section 5.2 we will discuss this result.

3.2. Bright field and isolated central galaxies

We proceed now to compare our samples of (bright) field and very isolated central galaxies. Recall that the latter is a subsample of the former. Fig. 6 shows $g - i$ color histograms for bright field (dotted lines) and isolated (solid lines) centrals in different stellar mass bins. The distributions are roughly similar in general. The chi-square test in this case shows probabilities above $P = 0.907$ that both normalized distributions are similar in each panel. Table 4 reports the fractions of blue central galaxies in bins of M_s corresponding to the distributions shown in Fig. 6. These fractions are close for both samples; if any, the isolated centrals show a

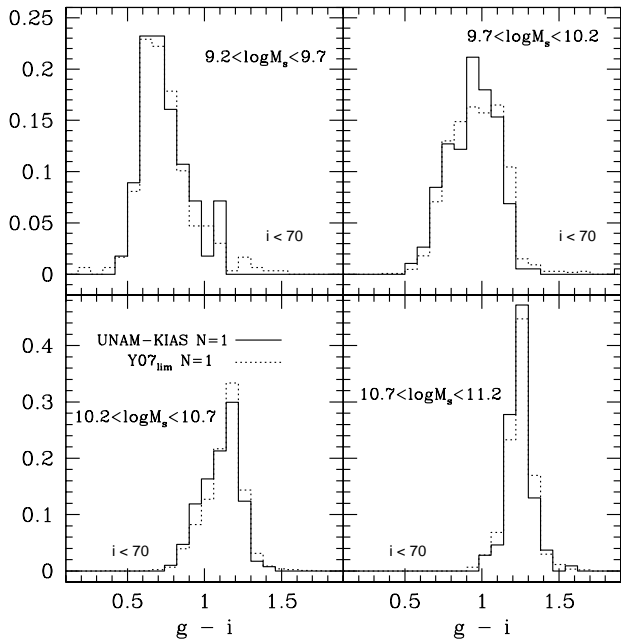


FIG. 6.— Histograms of $g-i$ color for bright field (dotted lines) and isolated (solid lines) central galaxies for different stellar mass bins (in units of $h^{-2} M_{\odot}$). We do not include objects with high inclination (angles over 70 degrees). Each histogram was normalized by the total number of selected objects, so that the sum of each distribution is equal to unity.

TABLE 5
RELATIVE FRACTIONS OF ACTIVE BRIGHT FIELD AND ACTIVE ISOLATED CENTRALS

$\log M_s$	sSFR cut	f_{active} bright field	f_{active} isolated
9.2–9.7	-10.5	0.83	0.80
9.7–10.2	-10.8	0.70	0.67
10.2–10.7	-11.2	0.43	0.50
10.7–11.2	-11.5	0.15	0.13

NOTE. — M_s bins as shown in Fig. 7. The second column is the cut in $\log(\text{sSFR}/\text{yrs}^{-1})$ to define an active/passive galaxy.

very marginal excess of blue galaxies with respect to the overall sample of bright field centrals, in particular at masses $9.7 < \log(M_s/h^{-2} M_{\odot}) < 10.7$, where the differences are of 6–7%. In the relatively low-mass bin, $9.7 < \log(M_s/h^{-2} M_{\odot}) < 10.2$ (right-top panel), while bright field centrals exhibit a slight bimodality with a red peak at $g-i = 1.1$, the distribution of isolated galaxies is narrower with a strong peak at $g-i = 0.9$. Both populations of $N = 1$ central galaxies are mainly red in the high-mass regime with a strong peak at $g-i \sim 1.3$.

In Fig. 7, the sSFRs distributions for the bright field and isolated centrals are plotted in the same M_s bins as in Fig. 6. Again the distributions are similar in general. The chi-square test confirms this with probabilities above $P = 0.945$ that both normalized distributions are similar in each panel. Table 5 reports the fractions of active central galaxies in bins of M_s corresponding to the distributions shown in Fig. 7. For intermediate masses (left-bottom panel), the fraction of active galaxies is higher in the isolated sample by 7% than in the bright field sample. The most massive regime (right-bottom panel) is dominated by passive galaxies in both samples.

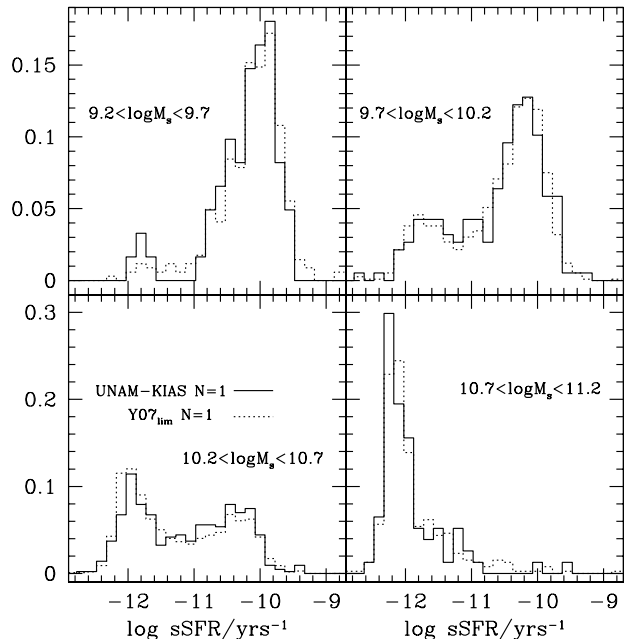


FIG. 7.— Histograms of specific star formation rate for bright field (dotted lines) and isolated (solid lines) central galaxies for different stellar mass bins (in units of $h^{-2} M_{\odot}$). Each histogram was normalized by the total number of selected objects, so that the sum of each distribution is equal to unity.

3.2.1. Gas-to-stellar mass ratios

Fig. 8 shows the gas-to-stellar mass ratio, M_{gas}/M_s , for isolated galaxies with available information on H I mass (see Section 2.2). They are split into two populations according to their sSFR; passive (red solid circles) and active (blue solid squares). The top panel shows the gas mass M_{gas} computed with the corrections for helium, metals, and H_2 mass (which depends on the morphological type T). Note that most of the galaxies with available H I information plotted in Fig. 8 have late-type morphologies ($T > 0$). The solid line in the panel is the fit of Avila-Reese et al. (2008) to a sample of local disk galaxies. In the case of elliptical galaxies, the M_{gas}/M_s ratios are much smaller. Isolated centrals have on average higher M_{gas}/M_s ratios compared to normal galaxies, for instance, by ~ 0.4 dex at $M_s \approx 5 \times 10^9 M_{\odot}$. The bottom panel shows the same as the top panel, but the gas mass is corrected only for helium and metals. The solid and dotted lines correspond to the fits of Stewart et al. (2009) and Papastergis et al. (2012) for compilations of observational data of disk galaxies, respectively. The dashed lines show the 1σ scatter according to Stewart et al. (2009). As before, we see that isolated centrals, especially the lower-mass ones, have higher M_{gas}/M_s ratios than normal disk galaxies, although the difference is smaller compared to the observed one in the top panel.

Isolated central galaxies have on average higher gas-to-stellar mass ratios than disk galaxies located in all environments, specially at lower masses. However, as shown in Section 3.2, the sSFR's of isolated galaxies at different masses do not differ significantly from those of bright field galaxies. This implies that isolated galaxies have larger gas reservoirs than galaxies in average envi-

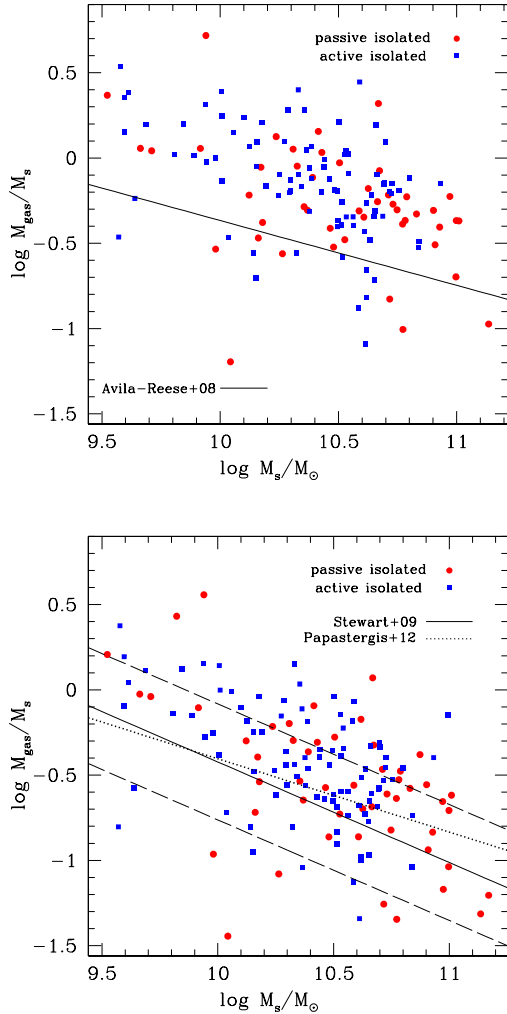


FIG. 8.— Gas-to-stellar mass ratio, M_{gas}/M_s , as a function of M_s (here $h = 0.7$) for isolated central galaxies. They are split into two populations according to their sSFR; passive (red solid circles) and active (blue solid squares). Top panel: We calculate M_{gas} using the approach by Avila-Reese et al. (2008) that takes into account helium, metals, and the mass of molecular hydrogen that depends on the morphology T . The solid line is the fit to their data. Bottom panel: M_{gas} is calculated using a correction for helium and metals, but mass of molecular hydrogen is not taken into account to be consistent with the equation (1) of Stewart et al. (2009, solid line). In addition, the dotted line is the fit of Papastergis et al. (2012) for observational estimates using H I mass. Both panels show that low-mass isolated galaxies have in general higher M_{gas}/M_s ratios than the average relations.

ronments but with similar levels of star formation activity. On the other hand, as can be seen in Fig. 8, the gas-to-stellar mass ratio of isolated centrals is somewhat independent if they are classified as active or passive star forming galaxies. A more detailed object-by-object analysis is necessary for confirming these results obtained here at a statistical level.

4. GALAXY-HALO MASS CONNECTION

In this Section we use the available halo mass information from Y07 for our samples of central galaxies (see details in Section 2.3). The top panel of Fig. 9 is the

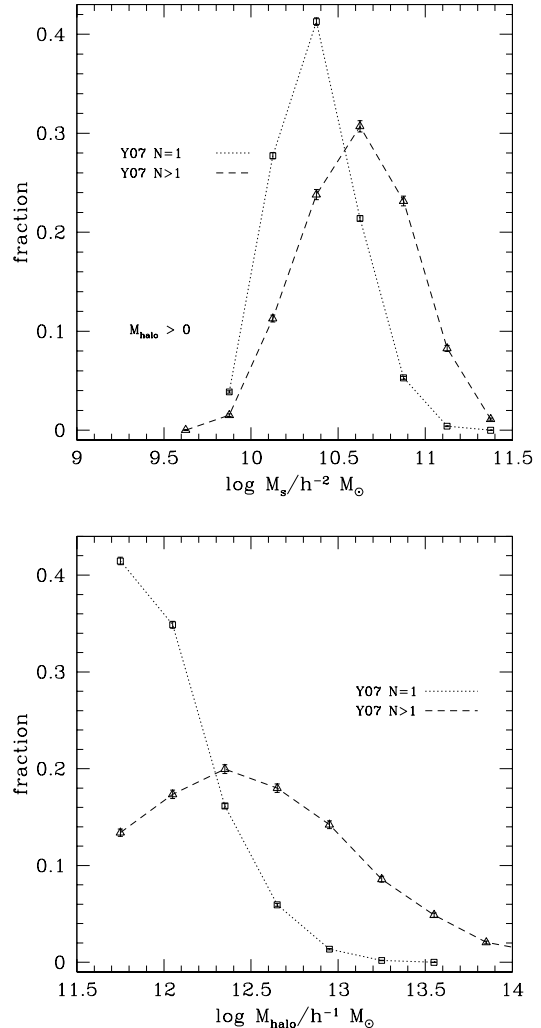


FIG. 9.— Top: Same as top panel of Fig. 1 but for central galaxies whose host halo mass is inferred by Y07. Bottom: Relative fraction as a function of host halo mass. At high halo masses, $\log(M_h/h^{-1} M_\odot) > 12.5$, the fraction of group centrals dominates with respect to that of field central galaxies.

same as the top panel of Fig. 1, but for central galaxies whose host halo mass is estimated by Y07. Since the determination of M_h for low-mass galaxies is difficult, there are fewer low-mass galaxies ($M_s < 10^{10} h^{-2} M_\odot$) than in Fig. 1 (see Table 1). However, the trend at high-masses ($M_s > 10^{10.5} h^{-2} M_\odot$) is still present; the relative fraction of group central galaxies is higher than that of field central objects. The chi-square test shows a very low probability of $P < 10^{-4}$ that both normalized distributions are similar.

The bottom panel shows the same relative fraction, but as a function of halo mass. The shape of the distributions among both samples are very different ($P < 10^{-7}$ that they are equal). Field ($N = 1$) central galaxies have a steep decrease in the relative fraction as M_h increases. The probability distribution to find a field central object in halos of $M_h > 10^{12.5} h^{-1} M_\odot$ is low. In the case of central galaxies in halos which host satellites (group centrals), they have a wide distribution in halo masses, with a long tail in the massive regime. The probability dis-

tribution to find a group central galaxy in halos of $M_h > 10^{12.5} h^{-1} M_\odot$ is relatively high in the local universe. It is well known that the halo mass correlates with the group/cluster richness (see e.g., Reyes et al. 2008, and the references therein).

We note that the relative fraction distribution of isolated central galaxies is similar to the one of bright field central galaxies, though the halo masses of the former are slightly smaller than those of the latter. Niemi et al. (2010) performed a study of isolated (elliptical) central galaxies using a Λ CDM-based catalog of simulated galaxies. They found that these galaxies reside in dark matter halos with masses lower than $\sim 2 \times 10^{13} h^{-1} M_\odot$, which is consistent with our results.

4.1. The M_s - M_h relation

In the last years, by means of statistical approaches and some direct measurements, the M_s - M_h relation at $z = 0$ and at higher redshifts has been inferred and used as a key constraint for models and simulations of galaxy evolution (e.g., Mandelbaum et al. 2006; Conroy & Wechsler 2009; Guo et al. 2010; Behroozi et al. 2010; Firmani & Avila-Reese 2010; Moster et al. 2010; More et al. 2011; Yang et al. 2012; Behroozi et al. 2013; Moster et al. 2013; Rodríguez-Puebla et al. 2013). This relation sheds light on the efficiency of galaxy (stellar) formation as a function of halo mass, and its scatter constrains the role of internal and halo evolutionary effects and of environment on the final stellar mass of galaxies. Since the effects of environment in isolated galaxies are in principle minimized, then the M_s - M_h relation of isolated galaxies should be associated mainly to intrinsic evolutionary processes. Does this relation differ from the one of all the galaxies? Does its scatter correlate with the main galaxy properties?

Here, we compare M_s vs. M_h for our samples of central galaxies separated into groups according to their properties. As a reference, we also compare our results with the fit to the M_s - M_h relation found in Yang et al. (2009) for the Y07 data of central galaxies including the 1σ scatter (the sample out to $z = 0.2$ has been used by these authors). The reported constant scatter in M_s around this relation is 0.173 dex, though as these authors discuss, at lower masses it seems to be smaller. For consistency, we use here the color separation into blue and red galaxies given by the same authors. They use the $^{0.1}(g-r)$ color (K -correction and evolution-correction at $z = 0.1$) with Petrosian magnitudes, which are measured within a circular aperture defined by the shape of the light profile. The $^{0.1}(g-r)$ color-magnitude criterion given in eq. (1) of Yang et al. (2008) is applied to select blue and red galaxies. For selecting passive and active galaxies, our eq. (4) is used. Furthermore, for the isolated centrals, we separate the sample into early- and late-type galaxies by the criterion $T < 0$ and $T > 0$, respectively.

In the main panels of Fig. 10 we plot the M_s - M_h relation for our very isolated galaxy sample, splitting it according to the color, sSFR, and morphological type T (left, middle and right panels, respectively). The median distribution for red, passive, and early-type galaxies is shown in red circles (red dashed lines), and that for blue, active and late-type galaxies is shown in blue squares (blue long-dashed lines). Error bars correspond

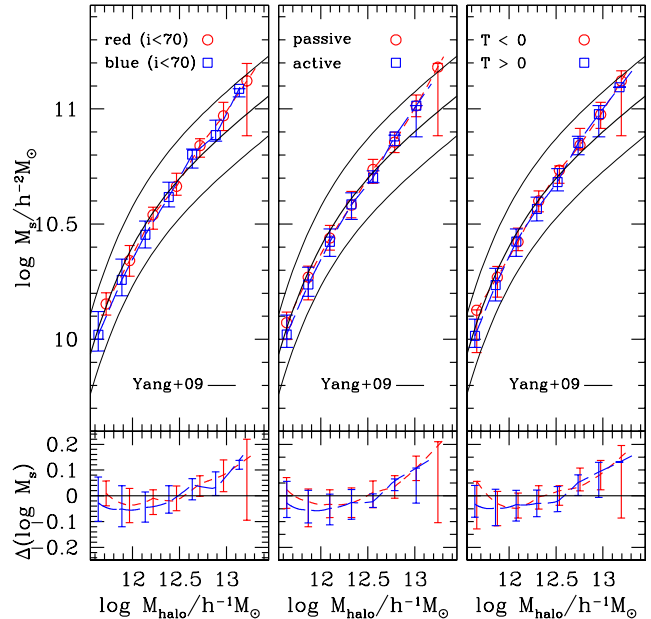


FIG. 10.— Stellar mass - halo mass relation for isolated central galaxies. They are split according to the color, sSFR and morphology (left, middle and right panels, respectively). The median distribution for red, passive and early-type galaxies is shown in red circles (red dashed lines), and that for blue, active and late-type galaxies is shown in blue squares (blue long-dashed lines). Error bars correspond to the 16 and 84 percentiles. M_s - M_h relations are very similar among these populations within the errors. The solid lines show the fit by Yang et al. (2009) to their data including the 1σ scatter. The lower box in each panel shows the residual in stellar mass, calculated as the difference between the median of each population and the fit by Yang et al. (2009), as a function of halo mass. Error bar corresponds to the dispersion of the median.

to the 16 and 84 percentiles. As can be seen from each panel, the M_s - M_h relations are similar within the errors. This means that the M_s - M_h relation of isolated galaxies is nearly independent of color, sSFR, and morphology. This result is obtained by using the halo mass based on the characteristic stellar mass. If we use M_h based on luminosity ranking, a very slight segregation by color in the M_s - M_h relation should appear but it is entirely due to the mass-to-light ratio dependence on color, and not due to something intrinsically related to the halo mass.

We compare the results in Fig. 10 with the fit to the M_s - M_h relation and its scatter found in Yang et al. (2009), which are shown as solid lines repeated in the main box of each panel. The scatter for our sample of isolated galaxies is clearly lower than 0.173 dex at all masses. The implications of this result will be discussed in Section 5.3. In addition, the lower box in each panel of Fig. 10 shows the residual in stellar mass, calculated as the difference between the median of each population and the fit by Yang et al. (2009), as a function of halo mass. Error bar corresponds to the dispersion of the median. The residuals show no differences among isolated galaxies of different properties (red/blue, passive/active or early-/late-type) within the errors, as already mentioned above.

According to Fig. 10, the M_s - M_h relation of very isolated galaxies is similar to that one of the overall sample of central galaxies in Y07 up to $M_h \sim 10^{12.5} h^{-1} M_\odot$.

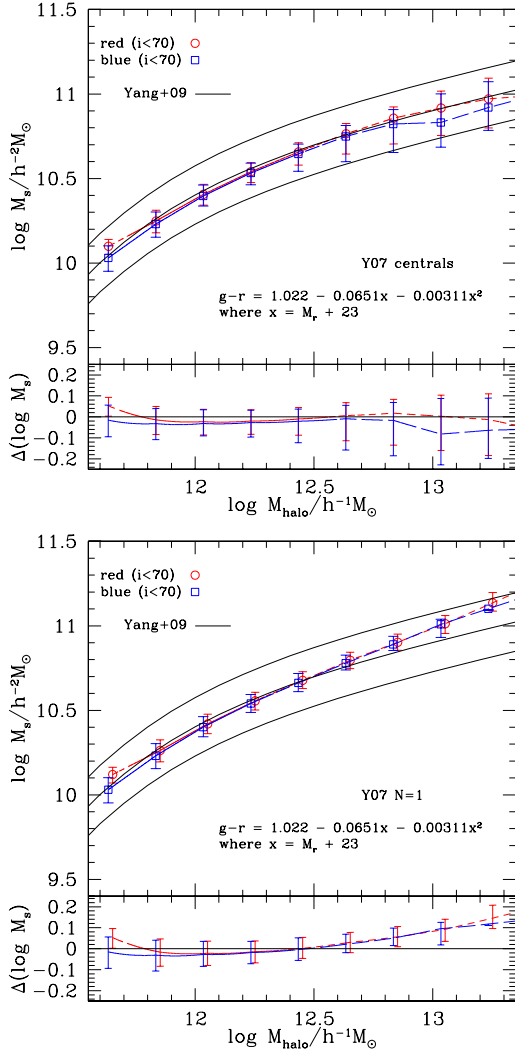


FIG. 11.— M_s – M_h relation for all (top panel) and field (bottom panel) central galaxies split by color. The median distribution for red galaxies is shown in red circles (red dashed lines), and that for blue galaxies is shown in blue squares (blue long-dashed lines). Error bars correspond to the 16 and 84 percentiles. The solid lines show the fit by Yang et al. (2009) to their data including the 1σ scatter. Note that their sample reaches $z = 0.2$, whereas our redshift limit is $z = 0.08$. The lower box in both panels shows the residual in stellar mass, calculated as the difference between the median of each population and the fit of Yang et al. (2009), as a function of halo mass. Error bars correspond to the dispersion of the medians. Field ($N = 1$) central galaxies show a higher residual compared to that of all ($N \geq 1$) central objects at high masses, which is independent of the galaxy property, e.g., color. This different behavior of the M_s – M_h relation is probably due to lack of systems without satellite galaxies in massive halos when assuming a one-to-one relation between total stellar mass and halo mass.

For larger masses, there is a systematic deviation of the isolated galaxies towards larger stellar masses as M_h is larger with respect to the overall sample of Y07 (out to $z = 0.2$). This means that at a given halo mass, the stellar masses of the isolated centrals are larger than those of the centrals in general. However, this is an expected result for centrals without satellites (our field $N = 1$ sample) in massive halos when using the method of Y07 to estimate the halo mass. Under the assumption of the one-to-one relation between total (characteristic) stellar

mass and halo mass, when only one galaxy inhabits a massive halo, i.e. the total stellar mass in the system is the stellar mass of this (central) galaxy, its M_s is larger than the mean for that halo mass. To the inverse, when more satellites are present in the massive halo, the stellar mass of the central galaxy is smaller. In Fig. 11 we plot the M_s – M_h relations (split by color) for our Y07-based sample (out to $z = 0.08$) of all central galaxies (field and group; upper panel), and for the field centrals ($N = 1$, lower panel) only. It is clearly seen that the M_s – M_h relation at large masses deviates from the average for the sample of $N = 1$ centrals, where the isolated ones are contained. In fact, it is rare to have only one galaxy in massive halos; they are populated typically by many galaxies (groups and clusters of galaxies). Instead, when centrals with $N > 1$ are included (they dominate in number at large masses), the median relation is very similar to the fit of Yang et al. (2009). Although the difference shown in Fig. 11 in the M_s – M_h relations for centrals in halos with $N = 1$ and $N > 1$ is mostly due to the method used to construct the group catalog, this may be still a valid result. For example, Niemi et al. (2010) found that, for a given halo mass, simulated isolated elliptical central galaxies (which on average correspond to systems with $N = 1$) contain more stellar mass with respect to simulated ellipticals in systems which roughly correspond to centrals in halos with $N > 1$.

We also see in Fig. 11 that the M_s – M_h relation of all the centrals or only the $N = 1$ (field) centrals is also the same for blue and red galaxies, as was the case for the isolated galaxies. Therefore, we conclude that *the M_s – M_h relation is nearly independent of the color for all kinds of central galaxies (group, field and isolated)*.

A caveat to be taken into account is that the halo masses we are using were estimated by applying the abundance matching of the total stellar (characteristic) and the halo cumulative mass functions. Strictly speaking, the abundance matching should be carried out separately for the blue and red stellar mass functions and the corresponding (unknown) halo mass functions of both populations. Under some assumptions, this exercise has been done in Rodríguez-Puebla et al. (2011). They have found that the M_s – M_h relations for blue and red central galaxies are indeed close, though with more notorious differences than those shown in Fig. 11.

Finally, according to the results shown in Figs. 10 and 11, the scatters of the M_s – M_h relations for the field centrals (including the isolated ones) seem to be lower than for the group central galaxies. However, we caution that the absolute values of the scatters are only lower limits due to the way the halo mass has been assigned in the Y07 catalog (see also Yang et al. 2008). We discuss further this topic in Section 5.3.

5. DISCUSSION

An exhaustive comparison among only central galaxies in some different environments was carried out. We compared the stellar and halo mass distributions among field and group centrals, and also between very isolated and bright field central galaxies. In addition, we compared their colors and sSFRs in the same stellar mass bins. It is important to note that unlike previous studies of this kind, in which galaxy properties are analyzed as a function of their environment without dis-

inction between centrals and satellites (for a review see Blanton & Moustakas 2009), or even in those works that separate galaxies into centrals and satellites to study the differences among the properties of both populations (e.g., Weinmann et al. 2006), our analysis have focused exclusively on central galaxies in different environments. Thus, it is difficult to compare our results with previous works. Following, we will discuss whether some of our results are consistent or not with previous studies of isolated galaxies or galaxies in systems with one or more satellites.

One of the remarkable differences between central galaxies in different environment is the stellar mass distribution. Field centrals ($N = 1$) dominate at the low-mass end, whereas group centrals ($N > 1$) dominate at the high-mass end. In this context, Trinh et al. (2013) used the NYU-VAGC catalog (based on SDSS DR6) to identify central galaxies in groups with $N = 1$ and $N = 2$. They found a higher fraction of centrals in halos with $N = 2$ with respect to centrals in halos with $N = 1$ at high stellar masses, which is consistent with our results.

On the other hand, Trinh et al. (2013) found a slight blue excess of 6% for centrals in systems with $N = 2$ relative to field centrals ($N = 1$) with the same stellar mass distribution using a sample with $M_r \leq -19$. This excess is consistent with our results but it is somewhat higher since we detect a very small excess of blue group centrals with respect to field centrals, around 1–5% (see Table 2). These authors defined red/blue galaxies using $g - r = 0.68$. If we use their condition in the $g - r$ color in addition to the cut $M_r \leq -19$, the population of red galaxies vanishes at very low masses (top-left panel in Fig. 3). We do not find any important excess of blue group central galaxies in systems with $N = 2$ (the differences are typically smaller than 4%), except the interval $9.6 < \log(M_s/h^{-2} M_\odot) < 10$ that shows a blue excess around 7% for centrals in systems with $N = 2$ relative to field centrals. The latter is in rough agreement with their results.

When comparing the subsample of very isolated galaxies with the sample of bright field galaxies (both with the same apparent magnitude limit), we do not find strong differences in their sSFR distributions. In agreement with our results, Kreckel et al. (2012) did not find strong differences in sSFR between low-mass SDSS galaxies (centrals and satellites) and a sample of galaxies in voids (large-scale regions of extreme low-density environment where most of the isolated galaxies could reside) with the same stellar mass. On the other hand, Rojas et al. (2005) and von Benda-Beckmann & Müller (2008) found that relatively bright galaxies in voids have slightly higher sSFR values than similar galaxies located in higher density environments. This is again in rough agreement with our results since our isolated central galaxies at intermediate masses ($10.2 < \log(M_s/h^{-2} M_\odot) < 10.7$) show slightly higher sSFR values than bright field galaxies (see Table 5). Note that the control samples in this kind of works correspond in general to central and satellites galaxies, whereas our comparison of isolated central galaxies was done only with respect to bright central galaxies in halos with $N = 1$, i.e., we do not include satellites galaxies nor central galaxies in halos hosting

also satellites.

5.1. Mass growth of central galaxies

We have seen that the mass distribution of group and field galaxies is different; 55% of the group centrals is found in the massive regime (stellar masses above the Milky Way), whereas this fraction is smaller than $\sim 20\%$ for the field centrals. Group central galaxies live typically in higher-density environments. As can be seen in the bottom panel of Fig. 9, most of these galaxies are located in massive host halos, which correspond to groups and clusters of galaxies. In this kind of environments, it is probable that the central galaxy suffered several mergers in the past, thus attaining higher stellar masses than the field galaxies. As the system (halo) grows up lately, the internal velocity dispersion increases in such a way that the merger probability of the remaining/new members becomes very low and today it remains as a system of many ($N > 1$) members in virial equilibrium.

On the other hand, the mass distribution of very isolated central bright galaxies is close to that of field bright centrals (both in systems with $N = 1$). Hirschmann et al. (2013) used a semi-analytic galaxy formation model based on Λ CDM cosmology and found that minor mergers provide a larger contribution to the overall stellar mass assembly of isolated galaxies as compared to major mergers. It is thought that minor mergers do not modify the morphology of the main galaxy. We check the morphological type for the isolated central galaxies with $M_s \geq 10^{10.5} h^{-2} M_\odot$ and find that those with $T \geq 1$ (late-type galaxies from Sa to Sm) dominate with 62%, whereas those with $T \leq -1$ (early-type galaxies from S0 to ellipticals) are just 31% of the sample at these masses (the remaining 7% corresponds to intermediate morphologies with $-1 < T < 1$). Thus, late-type morphologies are more common than early-type ones in our sample of massive isolated galaxies. This supports the idea that many of these galaxies increased their stellar masses partially by means of minor mergers, although there is also a fraction of early-type isolated galaxies that presumably grew through major mergers. It is plausible that a similar situation occurs with the massive centrals from the bright field sample, i.e., a dominant population of late-type galaxies at high stellar masses inhabiting relatively low-mass halos.

We conclude that centrals formed in halos rich in members ($N > 1$) are more probable to grow more in mass than those in halos with only one galaxy ($N = 1$, including the very isolated galaxies), probably due to more mergers. On the other hand, for massive centrals, a galaxy in a halo without satellites seems to have a smaller host halo mass than a galaxy of the same stellar mass but inhabiting a halo with many members. This may evidence that host halos of $N = 1$ or $N > 1$ centrals also have different growth (merger) histories. All this suggests that the stellar and halo merging of central galaxies within halos with many members ($N > 1$) should be different than those in halos without satellites ($N = 1$). However, in Section 3 we showed that, for a given stellar mass, there are no remarkable differences in properties such as color and sSFR among the central galaxies. Therefore, it seems that *the main galaxy properties and the evolution itself of central galaxies is dominated by internal processes rather than by the merger histories*

and environmental effects. We will study elsewhere the growth of central galaxies of equal stellar mass but with diverse halo assembly histories using numerical simulations.

5.2. Quenching of central galaxies

In Section 3 we presented observational results regarding the color and sSFR of the central galaxies. About 70–80% of field and group centrals at intermediate masses are red but there is a 30–50% of them with ongoing star formation. We have checked that $\sim 20\%$ of the field galaxies with $10^{10} < M_{star} < 10^{10.8} h^{-2} M_{\odot}$ are indeed classified as red but with high sSFR's. This fraction decreases to $\sim 15\%$ for group galaxies. It is in general assumed that the quenching (i.e., when a galaxy passes from star forming to passive) occurs in blue or green galaxies before they become red (and dead) objects. The fraction of red but active centrals at intermediate masses in our sample certainly do not follow this assumption. In addition, Mendel et al. (2013) identified a sample of young passive (quenched) galaxies from SDSS and found they are predominantly early-type objects, which suggests that the quenching is accompanied by morphological transformations in galaxies of the local universe (bear in mind that their sample includes central and satellite galaxies).

It is a very hard task to identify the physical processes behind the quenching, specially for central galaxies. Empirical and semi-empirical studies have shown that on average very massive galaxies were in the phase of quenching at high redshifts but with cosmic time, smaller galaxies become quenched (mass downsizing; e.g., Bundy et al. 2006; Drory & Alvarez 2008; Pozzetti et al. 2010; Firmani & Avila-Reese 2010). According to these studies, the typical stellar mass at which the transition to the passive regime happens at $z \sim 1$ and $z \sim 0$ is $6 - 7 \times 10^{10} M_{\odot}$ and $2 - 3 \times 10^{10} M_{\odot}$, respectively (see for instance, Fig. 8 in Firmani & Avila-Reese 2010 and more references therein). Peng et al. (2010, 2012) pointed out that different physical mechanisms may mimic their simple relation for the quenching rate of central galaxies, which is proportional to the SFR of them. On the other hand, Woo et al. (2013) used the SDSS to show that the fraction of quenched central galaxies is strongly correlated with halo mass at fixed stellar mass. This suggests that the quenching of a central galaxy is due to halo mass-depending mechanisms that prevent the cooling of infalling gas such as virial shock heating (Dekel & Birnboim 2006). Yang et al. (2013) support this picture by indicating that star formation in central galaxies is quenched once their halo masses reach a characteristic mass, which goes from $\sim 10^{12.5} h^{-1} M_{\odot}$ at $z > 3.5$ to $\sim 10^{11.5} h^{-1} M_{\odot}$ at $z = 0$. At larger halo masses, the gas is diluted and susceptible to AGN feedback.

The color transformation (from blue to red) should occur after quenching processes. The recent star formation activity in some field and group red central galaxies is perhaps due to interactions with other galaxies. It is known that star formation is moderately enhanced in galaxy pairs (e.g, Lambas et al. 2003; Hernández-Toledo et al. 2005), which extend out to projected separations of ~ 150 kpc (Patton et al. 2013), i.e., beyond the virial radius of low-mass halos. Central massive galaxies at $z = 0$ are the result of a tumultuous star

formation history at $z \geq 2$ but seem to follow a relatively quiet evolution since $z < 1$. Most of the local central galaxies at intermediate stellar masses have old stellar populations (hence red colors) after quenching processes. We conclude that for the fraction of those that have signs of recent star formation activity, it is plausible that this happens due to interactions between galaxies (for field and, in lower degree, group centrals with perturbers).

5.3. On the scatter of the M_s – M_h relation

The semi-empirical M_s – M_h relation has received a lot of attention in the last years since it summarizes many aspects of the efficiency of galaxy formation as a function of halo mass (see the references in Section 4.1). According to these studies (see also Figs. 10 and 11), at masses around $M_h \sim 10^{12} M_{\odot}$, the efficiency of stellar mass assembly is maximal; at lower masses it decreases, probably due to the stellar-driven (mainly Supernovae) negative feedback, as well as at larger masses, due to the long gas cooling times and AGN-driven negative feedback. All these processes are strongly dependent on the gravitational potential determined mainly by the halo mass. Therefore, the halo mass seems to be the main driver of the stellar mass growth of galaxies. Are other physical and evolutionary factors relevant, e.g., the halo mass aggregation history, the gas angular momentum, the environment, etc.?

Our analysis of only central galaxies presented in Section 4 has shown that: (i) The M_s – M_h relation of very isolated bright centrals does not differ from that of all field ($N = 1$) centrals. (ii) There is not a significant systematic difference in the M_s – M_h relation of central galaxies separated into blue and red (and into active and passive, and early- and late-types in the case of the isolated galaxies). (iii) The M_s – M_h relation of centrals with and without satellites ($N = 1$ and $N > 1$, respectively) are similar up to $M_h \sim 10^{13} h^{-1} M_{\odot}$; at larger masses, there are almost no centrals without satellites, but those few that are observed deviate systematically to larger stellar masses for their M_h than the $N > 1$ centrals; the latter is actually a consequence of assuming a one-to-one relation between total stellar mass and halo mass (see Section 4.1). Under the same assumption, the scatter of the M_s – M_h relation increases with halo mass for group central galaxies ($N > 1$), being minimal for field/isolated galaxies ($N = 1$).

The result that the scatter does not depend on color, sSFR or morphology may imply that all the physical and evolutionary processes that coin these internal properties are not important for the efficiency of galaxy stellar mass growth. Indeed, as shown in Section 3.2, once the stellar mass is fixed, the color and sSFR do not differ significantly between isolated and bright field centrals.

For the group central galaxies, neither the colors nor sSFRs differ significantly from those of field centrals for a given stellar mass. However, the scatter at large masses in the M_s – M_h relation seems to be higher for the group centrals. Under the assumption of a one-to-one relation between total stellar mass ($M_{s,tot}$) and halo mass, for a given M_h (and therefore $M_{s,tot}$), as smaller is the contribution of satellites to $M_{s,tot}$, the larger is the M_s of the central galaxy. Thus, it is expected that the scatter around the M_s – M_h relation at group/cluster scales is

partially due to this “mass partition” effect.

It is common to assign a scatter of ~ 0.17 dex to the M_s – M_h relation based mainly on inferences for group centrals, living in massive halos (c.f. Y07; Yang et al. 2009). However, as discussed above, *most of this scatter is dominated by conditions of the group establishment rather than by internal physical and evolutionary processes of the central galaxies*. The latter processes should produce a scatter in the M_s – M_h relation of field/isolated ($N = 1$) galaxies, which can be thought as the intrinsic component of the scatter around this relation in general. As mentioned above, Y07 calculated the group halo mass by assuming a one-to-one relation between the total stellar mass of the group and its halo mass (with no scatter in this relation), so that we cannot obtain conclusive results regarding the intrinsic scatter of the M_s – M_h relation by using this method. It should be very relevant to measure this intrinsic scatter, by means of statistical semi-empirical approaches (e.g., Rodríguez-Puebla et al. 2013) and/or by using the next weak lensing surveys, which puts strong constraints on models of galaxy evolution.

6. CONCLUSIONS

We have studied in detail the properties and distributions of central galaxies by using a catalog of very isolated galaxies (UNAM-KIAS collaboration, Hernández-Toledo et al. 2010) and a large halo-based galaxy group catalog (Y07), both constructed from the SDSS. Central galaxies were initially divided into two environments: those with satellite(s) inside the halo virial radius ($N > 1$, group centrals) and those without satellites ($N = 1$, field centrals). From the latter, we select the subsample of very isolated central galaxies, i.e. galaxies without perturber neighbors up to very large radii (likely much beyond the virial radius) according to strict 3D-isolation criteria. In order to compare adequately this subsample with the one of field galaxies, a subsample from the latter with the same apparent magnitude limit of the isolated centrals ($m_r < 15.2$) was selected (bright field centrals). In order to attain similar completeness limits and homogeneity, the four samples are limited to the same redshift range $0.01 \leq z \leq 0.08$, they are complete in M_s , and their galaxy properties were taken from the same analysis. Our main results are as follows:

- The stellar mass distributions of the field and group central galaxies are different (top panel of Fig. 1). The relative fraction of field and group central galaxies dominate at $M_s/h^{-2} M_\odot \sim 10^{10.4}$ and $10^{10.6}$, respectively. The differences in the mass distributions explain why the blue/star forming regions in the color– M_s and sSFR– M_s diagrams are populated mainly by field central galaxies, whereas the group central galaxies are mostly biased to the red/passive regions (Fig. 2). In the case of the isolated centrals, they do exhibit the same occupation in these diagrams compared to bright field central galaxies since both have similar stellar mass distributions.

- At parity of stellar mass (in the same M_s bins), the color distributions of the central galaxy samples are similar, specially between field and group centrals. If any, marginal differences arise at low-masses, where the relative fraction of blue group centrals is around 5% higher than that of blue field centrals. On the other hand, the relative fraction of blue isolated central galaxies is up

to barely $\sim 7\%$ higher than that of the blue bright field centrals at intermediate masses.

- The sSFR distributions of the central galaxy samples are also similar at parity of stellar mass, where bimodality is clearer than in the color distributions, specially for intermediate masses. When we use the stellar mass ratio between the most massive satellite and the central galaxy, μ_{21} , active group central galaxies with $\mu_{21} > 0.8$ peak at higher sSFR values than those with $\mu_{21} \leq 0.25$ for stellar mass bins in the interval $9.6 < \log(M_s/h^{-2} M_\odot) < 10.4$.

- The M_s – M_h relation of isolated galaxies (less affected by environment), shows no differences when they are separated by color, sSFR and morphological type T (using the halo mass based on the total stellar mass content). The same result is found for field centrals ($N = 1$) and group centrals ($N > 1$) separated by color.

- For isolated and field (both $N = 1$) galaxies, the M_s – M_h relation steepens at high halo masses with respect to group centrals; at these masses the probability to find a halo with a single member is actually low. This deviation is explained as a condition of the group when assuming a one-to-one relation between total stellar mass and halo mass (less members in a halo, more mass for the central galaxy) rather than by internal processes. Under the same assumption, the scatter around the M_s – M_h relation of group centrals ($N > 1$), which are mostly massive and living in massive halos ($> 10^{12.5} h^{-1} M_\odot$), increases systematically with M_h and it is likely higher than the scatter corresponding to isolated and field central galaxies (both $N = 1$). The absolute values of the scatters are only lower limits.

The general results from our study lead us to conclude that centrals assembled in dense environments (groups and clusters of galaxies) tend to have a stellar mass distribution biased to large masses ($M_s > 10^{10.6} h^{-2} M_\odot$), likely because they grew up significantly by mergers in the past, but after the velocity dispersion increases as the large halo relaxes, the probability of merging decreases and they remain as massive centrals surrounded by many satellite galaxies. In the case of the field ($N = 1$) centrals, most of them likely inhabit average environments in density (filaments/walls), where they have grown up less by mergers with the surrounding satellites, and may suffer the loss of some of them due to the tidal interactions with the larger structures in which their halos inhabit. Therefore, the mass distribution of field centrals tends to be biased to lower masses as compared with group centrals. In the case of the subsample of very (and bright) isolated galaxies, inhabiting probably in voids and the outskirts of walls and clusters, their mass distribution is similar to that of bright field galaxies, thus suggesting that both populations share comparable mass growth mechanisms.

The different mass distributions of the group and field centrals are behind the global differences of these samples in what regards their colors and sSFRs values. However, at a given M_s bin, there are only minor differences among the distributions of these properties for them. This implies that the mass growth of central galaxies is mostly driven by other factors and processes rather than the local environment and mergers.

The stellar mass growth efficiency of all the centrals

(given by the M_s -to- M_h ratio) is tightly related to their halo masses. This suggests that the halo mass is the main driver of central galaxy M_s growth. Disentangling the intrinsic scatter in the M_s - M_h relation of central galaxies without satellites will certainly help us to understand the internal processes that give rise to the galaxy properties and their connection with the evolution of halos.

ACKNOWLEDGMENTS

REFERENCES

- Aars, C. E., Marcum, P. M., & Fanelli, M. N. 2001, *AJ*, 122, 2923
- Adelman-McCarthy, J. K., Agüeros, M. A., Allam, S. S., Anderson, K. S. J., & et al. 2006, *ApJS*, 162, 38
- . 2007, *ApJS*, 172, 634
- Avila-Reese, V., Zavala, J., Firmani, C., & Hernández-Toledo, H. M. 2008, *AJ*, 136, 1340
- Behroozi, P. S., Conroy, C., & Wechsler, R. H. 2010, *ApJ*, 717, 379
- Behroozi, P. S., Wechsler, R. H., & Conroy, C. 2013, *ApJ*, 770, 57
- Bell, E. F., McIntosh, D. H., Katz, N., & Weinberg, M. D. 2003, *ApJS*, 149, 289
- Blanton, M. R. & Moustakas, J. 2009, *ARA&A*, 47, 159
- Blanton, M. R., Schlegel, D. J., Strauss, M. A., Brinkmann, J., Finkbeiner, D., Fukugita, M., Gunn, J. E., Hogg, D. W., Ivezić, Ž., Knapp, G. R., Lupton, R. H., Munn, J. A., Schneider, D. P., Tegmark, M., & Zehavi, I. 2005, *AJ*, 129, 2562
- Brinchmann, J., Charlot, S., White, S. D. M., Tremonti, C., Kauffmann, G., Heckman, T., & Brinkmann, J. 2004, *MNRAS*, 351, 1151
- Bundy, K., Ellis, R. S., Conselice, C. J., Taylor, J. E., Cooper, M. C., Willmer, C. N. A., Weiner, B. J., Coil, A. L., Noeske, K. G., & Eisenhardt, P. R. M. 2006, *ApJ*, 651, 120
- Conroy, C. & Wechsler, R. H. 2009, *ApJ*, 696, 620
- Dekel, A. & Birnboim, Y. 2006, *MNRAS*, 368, 2
- Drory, N. & Alvarez, M. 2008, *ApJ*, 680, 41
- Dutton, A. A., Conroy, C., van den Bosch, F. C., Simard, L., Mendel, J. T., Courteau, S., Dekel, A., More, S., & Prada, F. 2011, *MNRAS*, 416, 322
- Firmani, C. & Avila-Reese, V. 2010, *ApJ*, 723, 755
- Guo, Q., White, S., Li, C., & Boylan-Kolchin, M. 2010, *MNRAS*, 404, 1111
- Hearin, A. P., Zentner, A. R., Berlind, A. A., & Newman, J. A. 2013, *MNRAS*, 433, 659
- Hernández-Toledo, H. M., Avila-Reese, V., Conselice, C. J., & Puerari, I. 2005, *AJ*, 129, 682
- Hernández-Toledo, H. M., Vázquez-Mata, J. A., Martínez-Vázquez, L. A., Avila Reese, V., Méndez-Hernández, H., Ortega-Esbri, S., & Núñez, J. P. M. 2008, *AJ*, 136, 2115
- Hernández-Toledo, H. M., Vázquez-Mata, J. A., Martínez-Vázquez, L. A., Choi, Y.-Y., & Park, C. 2010, *AJ*, 139, 2525
- Hernández-Toledo, H. M., Zendejas-Domínguez, J., & Avila-Reese, V. 2007, *AJ*, 134, 2286
- Hirschmann, M., De Lucia, G., Iovino, A., & Cucciati, O. 2013, *MNRAS*, 433, 1479
- Karachentseva, V. E. 1973, *Astrofizicheskie Issledovaniia Izvestiya Spetsial'noj Astrofizicheskij Observatorii*, 8, 3
- Kreckel, K., Platen, E., Aragón-Calvo, M. A., van Gorkom, J. H., van de Weygaert, R., van der Hulst, J. M., & Beygu, B. 2012, *AJ*, 144, 16
- Lambas, D. G., Tissera, P. B., Alonso, M. S., & Coldwell, G. 2003, *MNRAS*, 346, 1189
- Mandelbaum, R., Seljak, U., Kauffmann, G., Hirata, C. M., & Brinkmann, J. 2006, *MNRAS*, 368, 715
- Márquez, I., Durret, F., González Delgado, R. M., Marrero, I., Masegosa, J., Maza, J., Moles, M., Pérez, E., & Roth, M. 1999, *A&AS*, 140, 1
- McGaugh, S. S. & de Blok, W. J. G. 1997, *ApJ*, 481, 689
- Mendel, J. T., Simard, L., Ellison, S. L., & Patton, D. R. 2013, *MNRAS*, 429, 2212
- More, S. 2012, *ApJ*, 761, 127
- More, S., van den Bosch, F. C., Cacciato, M., Skibba, R., Mo, H. J., & Yang, X. 2011, *MNRAS*, 410, 210
- Moster, B. P., Naab, T., & White, S. D. M. 2013, *MNRAS*, 428, 3121
- Moster, B. P., Somerville, R. S., Maulbetsch, C., van den Bosch, F. C., Macció, A. V., Naab, T., & Oser, L. 2010, *ApJ*, 710, 903
- Niemi, S.-M., Heinämäki, P., Nurmi, P., & Saar, E. 2010, *MNRAS*, 405, 477
- Papastergis, E., Cattaneo, A., Huang, S., Giovanelli, R., & Haynes, M. P. 2012, *ApJ*, 759, 138
- Pasquali, A., Gallazzi, A., Fontanot, F., van den Bosch, F. C., De Lucia, G., Mo, H. J., & Yang, X. 2010, *MNRAS*, 407, 937
- Patton, D. R., Torrey, P., Ellison, S. L., Mendel, J. T., & Scudder, J. M. 2013, *MNRAS*, 433, L59
- Peng, Y.-j., Lilly, S. J., Kovač, K., & et al. 2010, *ApJ*, 721, 193
- Peng, Y.-j., Lilly, S. J., Renzini, A., & Carollo, M. 2012, *ApJ*, 757, 4
- Pozzetti, L., Bolzonella, M., Zucca, E., Zamorani, G., Lilly, S., Renzini, A., Moresco, M., & Mignoli, M. 2010, *A&A*, 523, A13
- Press, W. H., Teukolsky, S. A., Vetterling, W. T., & Flannery, B. P. 1992, *Numerical recipes in C. The art of scientific computing* (Cambridge: University Press, —c1992, 2nd ed.)
- Reyes, R., Mandelbaum, R., Hirata, C., Bahcall, N., & Seljak, U. 2008, *MNRAS*, 390, 1157
- Roberts, M. S. & Haynes, M. P. 1994, *ARA&A*, 32, 115
- Rodríguez-Puebla, A., Avila-Reese, V., & Drory, N. 2013, *ApJ*, 767, 92
- Rodríguez-Puebla, A., Avila-Reese, V., Firmani, C., & Colín, P. 2011, *RMxAA*, 47, 235
- Rojas, R. R., Vogeley, M. S., Hoyle, F., & Brinkmann, J. 2005, *ApJ*, 624, 571
- Skibba, R. A., van den Bosch, F. C., Yang, X., More, S., Mo, H., & Fontanot, F. 2011, *MNRAS*, 410, 417
- Stewart, K. R., Bullock, J. S., Wechsler, R. H., & Maller, A. H. 2009, *ApJ*, 702, 307
- Trinh, C. Q., Barton, E. J., Bullock, J. S., Cooper, M. C., Zentner, A. R., & Wechsler, R. H. 2013, *MNRAS*, 436, 635
- van den Bosch, F. C., Aquino, D., Yang, X., Mo, H. J., Pasquali, A., McIntosh, D. H., Weinmann, S. M., & Kang, X. 2008, *MNRAS*, 387, 79
- Varela, J., Moles, M., Márquez, I., Galletta, G., Masegosa, J., & Bettoni, D. 2004, *A&A*, 420, 873
- Verdes-Montenegro, L., Sulentic, J., Lisenfeld, U., Leon, S., Espada, D., García, E., Sabater, J., & Verley, S. 2005, *A&A*, 436, 443
- Verley, S., Leon, S., Verdes-Montenegro, L., Combes, F., Sabater, J., Sulentic, J., Bergond, G., Espada, D., García, E., Lisenfeld, U., & Odewahn, S. C. 2007, *A&A*, 472, 121
- von Benda-Beckmann, A. M. & Müller, V. 2008, *MNRAS*, 384, 1189
- Weinmann, S. M., Kauffmann, G., van den Bosch, F. C., Pasquali, A., McIntosh, D. H., Mo, H., Yang, X., & Guo, Y. 2009, *MNRAS*, 394, 1213
- Weinmann, S. M., van den Bosch, F. C., Yang, X., & Mo, H. J. 2006, *MNRAS*, 366, 2

We thank the referee for the thoughtful comments and suggestions that helped to improve the paper. We thank José A. Vázquez-Mata for providing us the updated version of the UNAM-KIAS catalog. I.L. would like to thank Rut Salazar and Angel R. Calette for their technical support using CasJobs. I.L. acknowledges support from the Postdoctoral Fellowship program of DGAPA-UNAM, Mexico. A.R-P. and V.A-R acknowledge CONACyT (ciencia básica) grant 167332 for a terminal graduate student fellowship and for partial support. H.M.H.T acknowledges support from DGAPA-PAPIIT IN-112912 grant.

- Wetzel, A. R., Tinker, J. L., Conroy, C., & van den Bosch, F. C. 2013, *MNRAS*, 432, 336
- Woo, J., Dekel, A., Faber, S. M., Noeske, K., Koo, D. C., Gerke, B. F., Cooper, M. C., Salim, S., Dutton, A. A., Newman, J., Weiner, B. J., Bundy, K., Willmer, C. N. A., Davis, M., & Yan, R. 2013, *MNRAS*, 428, 3306
- Yang, X., Mo, H. J., & van den Bosch, F. C. 2008, *ApJ*, 676, 248
- . 2009, *ApJ*, 695, 900
- Yang, X., Mo, H. J., van den Bosch, F. C., Bonaca, A., Li, S., Lu, Y., Lu, Y., & Lu, Z. 2013, *ApJ*, 770, 115
- Yang, X., Mo, H. J., van den Bosch, F. C., & Jing, Y. P. 2005, *MNRAS*, 356, 1293
- Yang, X., Mo, H. J., van den Bosch, F. C., Pasquali, A., Li, C., & Barden, M. 2007, *ApJ*, 671, 153
- Yang, X., Mo, H. J., van den Bosch, F. C., Zhang, Y., & Han, J. 2012, *ApJ*, 752, 41